Journal of Organometallic Chemistry 902 (2019) 120957

Contents lists available at ScienceDirect

Journal of Organometallic Chemistry

journal homepage: www.elsevier.com/locate/jorganchem

Geometric isomerization and geometry controlled catalytic alcohol aminations of ruthenium hydride compounds containing bidentate pyrrolyl-imines

Yong-Jie Li [a], Hsuan-Ting Lai [a], Ching-Han Hu [a], Jie-Hong Chen [a], Chia-Her Lin [b], Jui-Hsien Huang [a, *]

[a] Department of Chemistry, National Changhua University of Education, Changhua, Taiwan, 50058
[b] Department of Chemistry, Chung-Yuan Christian University, Chun-Li, 320, Taiwan

ARTICLE INFO

Article history:
Received 24 April 2019
Received in revised form
19 September 2019
Accepted 25 September 2019
Available online 8 October 2019

Keywords:
Ruthenium
Pyrrole-imine
cis-trans isomerization
Hydrido

ABSTRACT

A series of ruthenium hydride compounds containing bidentate pyrrole-imine ligands were synthesized and characterized and their properties were fully studied. Reacting [C_4H_3NH-(2-CH=N-R) (**L_1H,** R = CH_2-2-furanyl; **L_2H**, R = CH_2-morpholine; **L_3H**, R = CH_2-2-pyridyl) with one equivalent of *n*-BuLi afforded the corresponding lithium reagents (**LiL_1~LiL_3**). Combining $RuHCl(CO)(PPh_3)_2$ with **LiL_1~LiL_3** in THF at 0 °C with stirring at room temperature for 12 h generated pure ***trans*-Pyr-Ru-H 1**−**3** in moderate yields after repeated fractional recrystallization. When the reactions were performed at reflux temperature, pure ***cis*-Pyr-Ru-H 1**−**3** were obtained by fractional recrystallization in relatively high yields. A thermal isomerization study showed that pure ***cis*-Pyr-Ru-H 1**−**3** and ***trans*-Pyr-Ru-H 1**−**3** can be interconverted in THF after refluxing and equilibrium was attained. Reacting a bulkier ligand [C_4H_3NLi-(2-CH=N-^tBu)] (**LiL_4**) with one equivalent $RuHCl(CO)(PPh_3)_3$ at room temperature afforded only ***cis*-Pyr-Ru-H 4** after purification. No ***trans*-Pyr-Ru-H 4** was observed, indicating the bulkier *t*-butyl group of the **L_4** ligand altered the stability of ***cis*-** and ***trans*-Pyr-Ru-H 4**. A catalytic alcohol amination study showed the *cis* forms of **Pyr-Ru-H** were the active catalysts for converting benzyl alcohol to *N*-benzylaniline.

1. Introduction

Ruthenium compounds are widely used as catalysts for dehydrogenation [1], arylation [2], transfer hydrogenation [3], alcohol amination [4], geometry isomerization [5], and for cancer cell growth inhibition reagents [6], etc. Among these ruthenium compounds, octahedral geometries of ruthenium complexes containing hydride, carbonyl, and varieties of ligands represent an important series of catalysts and several review papers regarding the corresponding ruthenium hydride compounds have been published [7]. The relative positions of ancillary ligands and hydride on the ruthenium atom may confer different catalytic activities to these ruthenium compounds. Therefore, the geometries and thermal stability of ruthenium hydride [8] compounds are important factors in the study of catalytic reactions using these ruthenium hydride compounds.

$RuHCl(CO)(PPh_3)_3$ (**1**) [9] is a common starting material for synthesizing corresponding compounds with ancillary ligands. Reacting **1** with asymmetric bidentate C~N, N~N, N~O ligands (L~L′) generated $RuH(L\sim L')(CO)(PPh_3)_2$ which may contain *trans*- and *cis*-P-Ru-P [10] types of geometries as shown in Scheme 1. In searching the Cambridge Crystal Structure Database, we found most of the related geometries of $RuH(L\sim L')(CO)(PPh_3)_2$ are the *trans*-P-Ru-P type and only a few are the *cis*-P-Ru-P type [11]. Among the *trans*-P-Ru-P type of $RuH(L\sim L')(CO)(PPh_3)_2$ compounds, some asymmetrical bidentate N~N′ ligands were used to generate a series of $RuH(N\sim N')(CO)(PPh_3)_2$ compounds [12]. It is known that the hydride group of these ruthenium compounds may be arranged in either *trans* or *cis* position relative to one of the nitrogen atoms of the N~N' ligand and sometimes both geometries can be obtained simultaneously, as shown in Scheme 1(a). These observations led us to examine the questions: (i) can the two isomers be separated; (ii) can the two isomers be interconverted to each other; and (iii) which isomer is the active form for catalytic alcohol amination? Here we report the synthesis of a series of ruthenium hydride

* Corresponding author.
E-mail address: juihuang@cc.ncue.edu.tw (J.-H. Huang).

https://doi.org/10.1016/j.jorganchem.2019.120957
0022-328X/

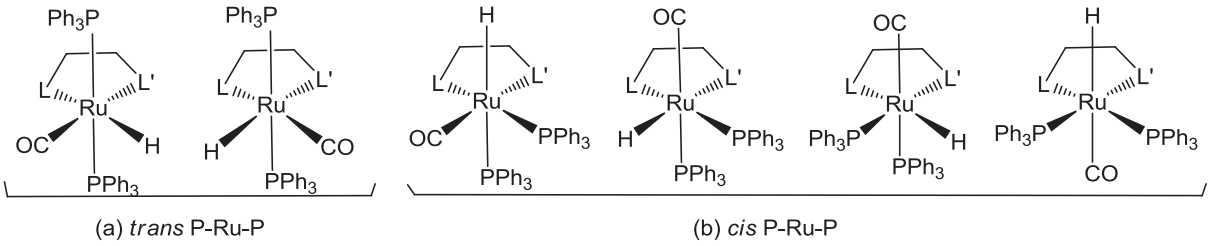

Scheme 1. Possible geometries of Ru(L~L′)HCl(CO)(PPh_3)$_2$ where the two PPh_3 fragments are arranged as (a) *trans* and (b) *cis* form.

compounds containing asymmetrical bidentate pyrrole-imine ligands. We discuss their geometries, thermal isomerization, and their abilities to catalyze alcohol aminations.

2. Results and discussion

2.1. Synthesis and characterization of compounds trans- and cis-Pyr-Ru-H 1–3 and cis-Pyr-Ru-H 4

The bidentate pyrrole-imine ligands **L_1H~L_4H** (**L_1H**, R = -CH_2-2′-furanyl; **L_2H**, R = -CH_2CH_2-morpholine; **L_3H**, R = -CH_2-2′-pyridinyl, **L_4H**, R = -^{t}Bu) were prepared easily according to the published procedures [13] by reacting pyrrole-2-carboxaldehyde with an equimolar amount of amines in methanol. The pyrrole-imine ligands **L_1H~L_3H** were converted to their corresponding lithium salts (**LiL_1~LiL_3**) with *n*-BuLi in THF and with the consecutive addition of those lithium salts to THF solutions of RuH(CO)Cl(PPh_3)$_3$ at 0 °C. The solutions were stirred at room temperature under nitrogen for 12 h generating RuH(CO)(PPh_3)$_2$[C_4H_3N(2-CH=NR)] (***trans*-Pyr-Ru-H 1**, R = -CH_2-2′-furanyl; ***trans*-Pyr-Ru-H 2**, R = -CH_2CH_2-morpholine; ***trans*-Pyr-Ru-H 3**, R = -CH_2-2′-pyridinyl) in moderate yields after filtration through Celite to remove LiCl, washing with heptane to remove excess PPh_3, and repeated fractional recrystallization (Scheme 2). Here the ***trans*-Pyr-Ru-H** and ***cis*-Pyr-Ru-H** were defined based on the relative position of the hydride and pyrrolyl fragments.

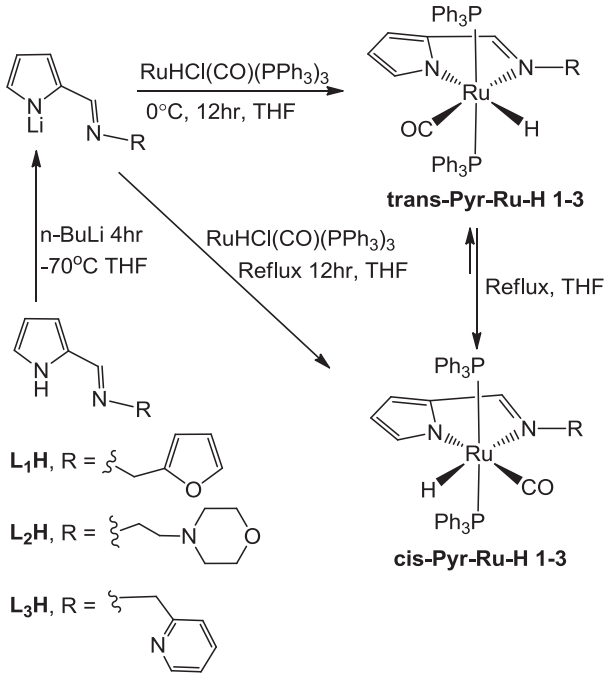

Scheme 2. Synthesis of complexes ***cis*-Pyr-Ru-H 1–3** and ***cis*-Pyr-Ru-H 1–3**.

The ^{1}H, ^{13}C and ^{31}P NMR and IR spectra of ***trans*-Pyr-Ru-H 1–3** were measured. The signals of ruthenium hydride for compounds ***trans*-Pyr-Ru-H 1–3** appeared as a triplet at *ca.* δ −11.3 with $^2J_{PH}$ at *ca.* 19 Hz, representing the two PPh_3 ligands located *cis* to the Ru-*H* [4c,12,14]. The ^{13}C NMR spectra of all compounds showed a triplet at *ca.* δ 206 for the CO group [15] with $^2J_{C\text{-}P}$ coupling constants at 14–17 Hz. The phenyl C_{ipso} carbon of PPh_3 showed typical virtual coupling [16] with the $^1J_{P\text{-}C}$ at ca. 20 Hz. The ^{1}H NMR and ^{13}C NMR signal for the methine of imine CH=N fragment showed a single resonance in the range of δ 7.52–6.29 and δ 159.6–153.7, respectively. The results were confirmed by ^{1}H-^{13}C NMR 2D NMR spectroscopy (see supporting information, shows only the NMR spectra of ***trans*-Pyr-Ru-H 1**).

It is worth noting that adding **LiL_1-LiL_3**/THF solutions to RuH(CO)Cl(PPh_3)$_3$/THF solution under nitrogen and heating at 70 °C for 24 h afforded RuH(CO)(PPh_3)$_2$[C_4H_3N(2-CH=NR)] (***cis*-Pyr-Ru-H 1**, R = -CH_2-2′-furanyl; ***cis*-Pyr-Ru-H 2**, R = -CH_2CH_2-morpholine; ***cis*-Pyr-Ru-H 3**, R = -CH_2-2′-pyridinyl) in moderate yields after filtration and recrystallization as shown for the synthesis of ***trans*-Pyr-Ru-H 1–3**. The ^{1}H, ^{13}C, and ^{31}P NMR resonance patterns of ***cis*-Pyr-Ru-H 1–3** were very similar to those of ***trans*-Pyr-Ru-H 1–3**. The ruthenium hydride chemical shifts in $CDCl_3$ for compounds ***cis*-Pyr-Ru-H 1–3** appeared at *ca.* δ −10.74 ~ −10.93 with $^2J_{PH}$ at *ca.* 22 Hz, and the ^{31}P NMR showed resonance at *ca.* δ 47.0.

2.2. Thermal isomerization of trans- and cis-Pyr-Ru-H compounds

The geometries of ruthenium hydrides containing multidentate ligands can affect their catalytic activity toward reactants. This is due to different ligands restrict the reactants approaching the metal centers. Therefore, many ruthenium hydrides have been structurally characterized. Among these compounds, only limit examples show the interconversion of their geometries under certain conditions [17]. Interestingly, the pure ***trans*-** and ***cis*-Pyr-Ru-H 1–3** can interconvert thermodynamically. When solutions of ***trans*-Pyr-Ru-H 1** (Fig. 1a) and ***cis*-Pyr-Ru-H 1** (Fig. 1c) in C_6D_6 were heated in J-Young NMR tubes for 8 h at 70 °C, both solutions reached equilibrium with the K_{eq}, (298*K*) at 12.8 (Fig. 1b and d). The conversion rates of ***trans*-Pyr-Ru-H 1** to ***cis*-Pyr-Ru-H 1** were measured by using ^{1}H NMR spectra for recording the conversion rates. The k_{obs} were obtained from the plot of time (sec) vs conversion. By using k_{obs} vs temperature, we can calculate the 1/T and ln(k_{obs}/T) (Table 1) and generate an Erying plot as shown in Fig. 2. The $\Delta H^{\ddagger}$ and $\Delta S^{\ddagger}$ were estimated at 29.5 kcal/mol and 8.86 cal K/mol, respectively. Theoretical calculations of the relative energy (in terms of total enthalpy at 298 K) of ***trans*-** and ***cis*-Pyr-Ru-H 1–3** were obtained with the M06-2X functional [18], along with 6-31G(d)-basis set for C, H, O, N, and LANL2DZ for Ru. Solvation effects of THF were included using the conductor-like polarizable continuum model

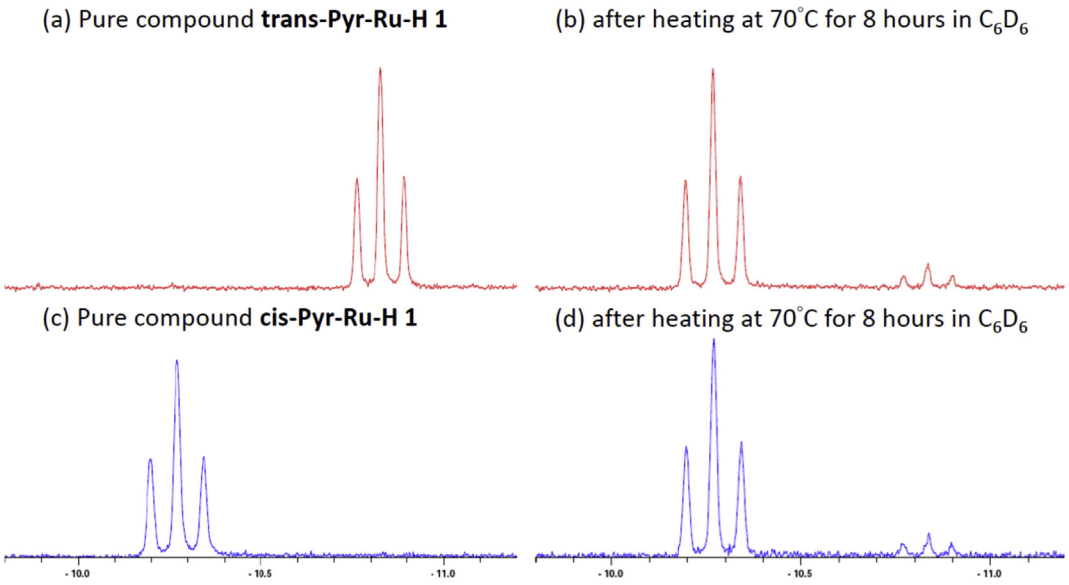

Fig. 1. Thermal interconversion of compounds ***trans*-Pyr-Ru-H 1** and ***cis*-Pyr-Ru-H 1**. (a) and (c): ^{1}H NMR spectra of hydride region of pure compounds ***trans*-Pyr-Ru-H 1** and ***cis*-Pyr-Ru-H 1**, respectively; (b) and (d), after heating at 70 °C for 8 h in C_6D_6.

Table 1
The Eyring plot of thermal conversion of compound *trans*-Pyr-Ru-H 1 to *cis*-Pyr-Ru-H 1 in C_6D_6.

Temp (K)	k_{obs}	$1/T$	$\mathrm{Ln}(k_{obs}/T)$
328	1.34×10^{-5}	3.05×10^{-3}	−17.01
333	3.00×10^{-5}	3.00×10^{-3}	−16.22
338	6.27×10^{-5}	2.96×10^{-3}	−15.50
343	9.92×10^{-5}	2.92×10^{-3}	−15.06
348	2.04×10^{-4}	2.87×10^{-3}	−14.35

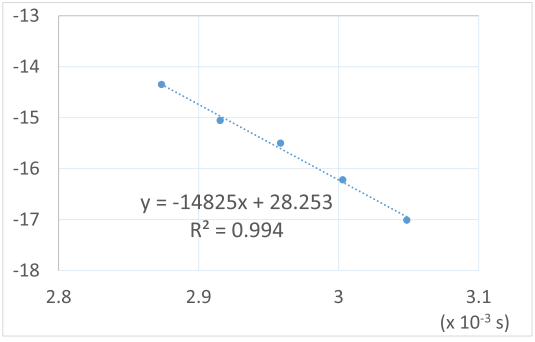

Fig. 2. The Eyring plot for the conversions of ***trans*-Pyr-Ru-H 1** to ***cis*-Pyr-Ru-H 1**. X axis, the values of 1/T; Y, the values of $ln(k_{obs}/T)$.

(CPCM) approach [19]. The Gaussian 09 suite of programs was used in our studies [20]. Geometry optimizations and harmonic vibrational frequencies were performed using the CPCM analytic gradients. The vibrational frequencies were utilized to compute thermodynamic corrections to enthalpies at 298 K. The relative energies of ***cis* Pyr-Ru-H 1–3** were all lower than those of their ***trans*-Pyr-Ru-H 1–3** counterparts (Table 2). The results were consistent with the experimental data showing that the ***cis* Pyr-Ru-H** form is much more stable than the ***trans*-** ones. Presumably, the stereo geometry arrangement of *cis* form has less steric hindrance and lower the energy.

2.3. Molecular geometries of trans-Pyr-Ru-H 1–2 and cis-Pyr-Ru-H 1-3

Even though the compounds ***trans*- and *cis*-Pyr-Ru-H 1–3** were characterized by NMR spectroscopy, the relative positions of the pyrrole, imine, hydride, carbonyl and two PPh_3 were still unclear. Structure determination was quite important to understand their geometries, thermal stabilities, and reactivities. The crystals of ***trans*-Pyr-Ru-H 1–2** and ***cis*-Pyr-Ru-H 2–3** were obtained by dissolving these compounds in methylene chloride and with careful layering with dimethylsulfoxide. The crystals of ***cis*-Pyr-Ru-H 1** were obtained from a methylene chloride/heptane mixed solution. The geometries of ***trans*-Pyr-Ru-H 1–2** and ***cis*-Pyr-Ru-H 1–3** are shown in Figs. 3–7 and their data collection and selected bond lengths and angles are listed in Tables 3 and 4, respectively. All the geometries of ***trans*-Pyr-Ru-H 1–2** and ***cis*-Pyr-Ru-H 1–3** displayed an octahedral geometry. The geometries of ***trans*-Pyr-Ru-H 1–2** showed that the two nitrogen atoms of bidentate pyrrole-imine took the *cis* positions in an equatorial plane where the pyrrole fragment was *trans* to the hydride and the imine fragment was *trans* to the carbonyl group. The remaining two PPh_3 ligands mutually occupied the *trans* positions. The geometries of ***cis*-Pyr-Ru-H 1–3** were very like the geometries of ***trans*-Pyr-Ru-H** isomers except the pyrrole fragment was *trans* to the carbonyl and the imine fragment was *trans* to the hydride, resulting in the pyrrole fragment being *cis* to the hydride. The bond lengths of Ru to pyrrolyl and imine were all very similar to those of ***trans*-Pyr-Ru-H 1–2** and ***cis*-Pyr-Ru-H 1–3**, consistent with the results reported in the literature [21]. However, our findings revealed some important information regarding these structures: (i) the trans form has a lower C-O stretching frequency than the cis form, it seems that the imine group is a better donor than the pyrrolyl and (ii) the linearity of P-Ru-P was highly dependent on the geometries of the bidentate pyrrole-imine *verses* the hydride and the CO groups where the ***trans*-Pyr-Ru-H 1–2** presented a larger bonding angle (>170°) than those of **the *cis*-Pyr-Ru-H 1–3** variant (<170°).

Table 2
Theoretical calculation of formation energy of ***cis*- and *trans*-Pyr-Ru-H 1–4**.

compound	Formation energy (hartrees)	ΔH Formation energy (KJ/mol)
***cis*-Pyr-Ru-H 1**	−2849.8303	2.28
***trans*-Pyr-Ru-H 1**	−2849.8292	
***cis*-Pyr-Ru-H 2** ***trans*-Pyr-Ru-H 2**	−2946.7609	6.30
	−2946.7585	
***cis*-Pyr-Ru-H 3** ***trans*-Pyr-Ru-H 3**	−2868.0638	23.10
	−2868.0550	
***cis*-Pyr-Ru-H 4**	−2738.9348	16.28
***trans*-Pyr-Ru-H 4**	−2738.9322	

*A hartree is equal to 2625.5 kJ/mol.

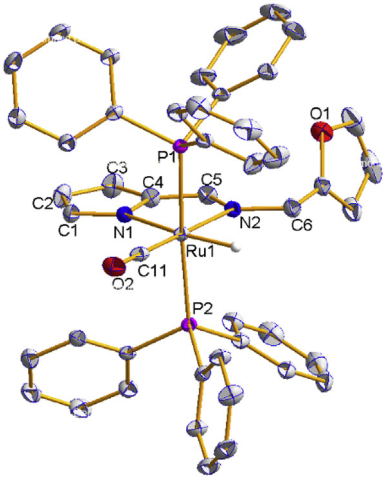

Fig. 3. Molecular geometry of ***trans*-Pyr-Ru-H 1**. The hydrogen atoms except the hydride were omitted for clarity. Thermal ellipsoids were drawn at 30% probabilities.

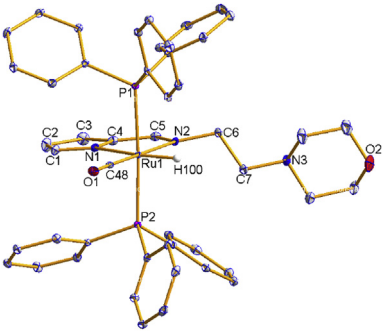

Fig. 4. Molecular geometry of ***trans*-Pyr-Ru-H 2**. The hydrogen atoms except the hydride were omitted for clarity. Thermal ellipsoids were drawn at 30% probabilities.

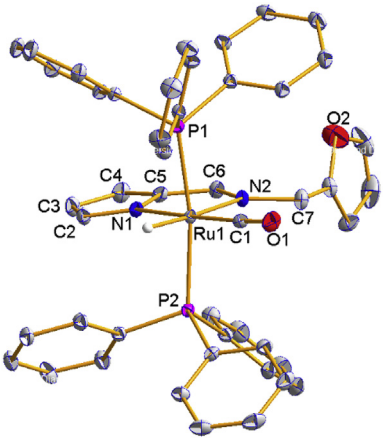

Fig. 5. Molecular geometry of ***cis*-Pyr-Ru-H 1**. The hydrogen atoms except the hydride were omitted for clarity. Thermal ellipsoids were drawn at 30% probabilities.

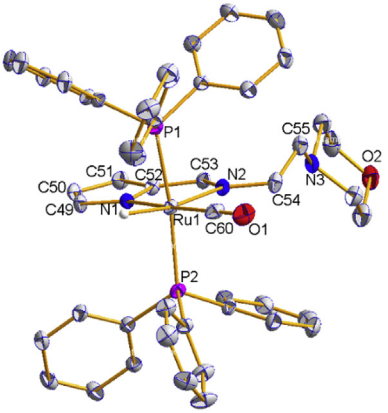

Fig. 6. Molecular geometry of ***cis*-Pyr-Ru-H 2**. The hydrogen atoms except the hydride were omitted for clarity. Thermal ellipsoids were drawn at 30% probabilities.

2.4. The effect of a bulky imine substituent–synthesis and characterization of cis-Pyr-Ru-H 4

In the beginning of this research, only primary amines were used for the ligand synthesis, *i.e.*, only **L_1H~L_3H** were used. From the experimental data, we learned that the ***cis*-Pyr-Ru-H 1–3** isomers were more thermally stable than the ***trans*-Pyr-Ru-H 1–3** isomers. Even though their bond angles and lengths were quite similar, after carefully comparing these geometries, we noted that the bond angles of P-Ru-P for the ***cis*-Pyr-Ru-H 1–3** (ca.169°) were smaller than those of ***trans*-Pyr-Ru-H 1–2** (ca. 173-176°). Presumably, the steric hindrance of the imine substituents affected the geometry arrangement of ***trans*-Pyr-Ru-H** and ***cis*-Pyr-Ru-H** isomers. With relation to this, the greater steric hindrance of *t*-butyl amine was used to form a bidentate pyrrole-imine ligand **L_4H** and to synthesize its corresponding ruthenium compound as shown in Scheme 3. When **L_4H** was used to react with *n*-BuLi in THF and with consecutive addition of the **LiL_4**/THF solution to a THF solution of RuH(CO)Cl(PPh_3)$_3$ at 0 °C with stirring at room temperature under nitrogen for 12 h, only RuH(CO)(PPh_3)$_2$[C_4H_3N(2-CH=N^{t}Bu)] (***cis*-Pyr-Ru-H 4**) was isolated in 74% yield (Scheme 3). No ***trans*-Pyr-Ru-H 4** was found in the reaction products. These results indicated that the bulky imine substituent raised the formation energy of ***trans*-Pry-Ru-H 4** and lowered the formation energy of ***cis*-Pyr-Ru-H 4** as

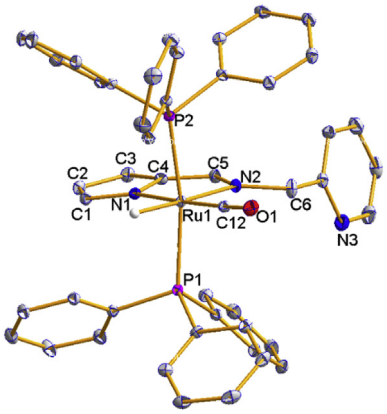

Fig. 7. Molecular geometry of ***cis*-Pyr-Ru-H 3**. The hydrogen atoms except the hydride were omitted for clarity. Thermal ellipsoids were drawn at 30% probabilities.

shown in Table 2. The ^{1}H NMR spectra of ***cis*-Pyr-Ru-H 4** showed a triplet at −12.08 with $^{2}J_{P\text{-}H}$ at 23 Hz assigned as the Ru-H. The ^{13}C NMR spectrum of ***cis*-Pyr-Ru-H 4** showed a triplet at *ca* δ 207.6 for the CO group with $^{2}J_{C\text{-}P}$ coupling constant at 13 Hz. Heating ***cis*-Pyr-Ru-H 4** in C_6D_6 in a J-Young NMR tube at elevated temperature did not establish an equilibrium between ***trans*-** and ***cis*-Pyr-Ru-H 4** in the solution. The yellowish crystals of ***cis*-Pyr-Ru-H 4** were obtained from a THF and heptane mixed solvent at −20 °C. Crystal data and selected bond lengths and angles are listed in Tables 3 and 4 and its molecular geometry is shown in Fig. 8. The geometry of ***cis*-Pyr-Ru-H 4** is similar to ***cis*-Pyr-Ru-H 1**−**3** and can be described as a distorted octahedral. Their bond lengths and angles were quite similar. However, while comparing the geometry and bonding angles of ***cis*-Pyr-Ru-H 4** with ***cis*-Pyr-Ru-H 1**−**3**, we found that the P(1)-Ru(1)-P(2) is at 161.71(5)°, much smaller than those for ***cis*-Pyr-Ru-H 1**−**3**. The results further proved the previous assumption that the steric bulkiness of the substituted imine R group may alter

Table 3
Summary of crystallographic data for ***trans*-Pyr-Ru-H 1**−**2** and ***cis*-Pyr-Ru-H 1~4**.

	trans-Pyr-Ru-H 1	*trans*-Pyr-Ru-H 2	*cis*-Pyr-Ru-H 1
formula	$C_{47}H_{40}N_2O_2P_2Ru$	$C_{49}H_{49}Cl_2N_3O_2P_2Ru$	$C_{47}H_{40}N_2O_2P_2Ru$
FW	827.82	945.82	827.82
T [K]	150	100	150
Crystal system	Triclinic	Triclinic	Triclinic
space group	P-1	P-1	P-1
a [Å]	11.720(3)	10.1825(11)	10.4546(6)
b [Å]	12.369(3)	12.0355(13)	12.3797(7)
c [Å]	16.202(4)	18.613(2)	17.0623(10)
α [°]	73.898(12)	89.713(6)	106.398(3)
β [°]	75.231(12)	77.152(6)	97.897(3)
γ [°]	62.691(10)	82.980(6)	108.112(3)
V [Å^3]	1982.5(8)	2206.7(4)	1951.1(2)
Z	2	2	2
ρ_c [Mg m^{-3}]	1.385	1.423	1.409
μ[mm-^{1}]	0.517	0.592	0.526
F(000)	850	976	852
rflns collected	34518	32029	39152
independent rflns	10174 [$R_{int} = 0.0415$]	10924 [$R_{int} = 0.0538$]	10093 [$R_{int} = 0.0467$]
data/restraints/parameters	10174/0/491	10924/0/536	10093/0/491
goodness-of-fit on F^2	0.888	1.037	0.887
R_1, wR_2 ($I > 2\sigma(I)$)	$R_1 = 0.0367$, w$R_2 = 0.1117$	$R_1 = 0.0384$, w$R_2 = 0.0917$	$R_1 = 0.0376$, w$R_2 = 0.1128$
R_1, wR_2(all data)	$R_1 = 0.0502$, w$R_2 = 0.1317$	$R_1 = 0.0482$, w$R_2 = 0.0979$	$R_1 = 0.0486$, w$R_2 = 0.1256$
largest diff. peak, hole [*e*Å^{-3}]	0.479/-1.466	0.944/-0.899	0.741/-0.958
	cis-Pyr-Ru-H 2	*cis*-Pyr-Ru-H 3	*cis*-Pyr-Ru-H 4
formula	$C_{48}H_{47}N_3O_2P_2Ru$	$C_{48}H_{41}N_3OP_2Ru$	$C_{46}H_{44}N_2OP_2Ru$
FW	860.89	838.84	803.89
T [K]	100(2)	150(2)	100(2)
Crystal system	Monoclinic	Triclinic	Monoclinic
space group	$P2_1/n$	P-1	$P2_1/c$
a [Å]	12.758(3)	10.5045(4)	18.041(10)
b [Å]	23.499(5)	12.4650(5)	12.436(7)
c [Å]	14.075(3)	16.9596(6)	18.913(9)
α [°]	90	106.029(2)	90
β [°]	90.796(15)	97.669(2)	112.28(3)
γ [°]	90	109.256(2)	90
V [Å^3]	4219.3(16)	1952.27(14)	3927(4)
Z	4	2	4
ρ_c [Mg m^{-3}]	1.355	1.425	1.358
μ[mm-^{1}]	0.490	0.525	0.518
F(000)	1784	862	1660
rflns collected	39929	38134	55156
independent rflns	9843 [$R_{int} = 0.1282$]	10114 [$R_{int} = 0.0503$]	10018 [$R_{int} = 0.1770$]
data/restraints/parameters	9843/0/505	10114/0/500	10018/0/476
goodness-of-fit on F^2	0.785	0.864	0.962
R_1, wR_2 ($I > 2\sigma(I)$)	$R_1 = 0.0564$, w$R_2 = 0.1022$	$R_1 = 0.0384$, w$R_2 = 0.1128$	$R_1 = 0.0686$, w$R_2 = 0.1631$
R_1, wR_2(all data)	$R_1 = 0.1174$, w$R_2 = 0.1180$	$R_1 = 0.0509$, w$R_2 = 0.1265$	$R_1 = 0.1349$, w$R_2 = 0.2001$
largest diff. peak, hole [*e*Å^{-3}]	0.849/-0.605	0.826/-0.686	1.314/-2.174

Table 4
Selected Bond lengths (Å) and angles (°) for compounds ***trans*-Pyr-Ru-H 1–2** and ***cis*-Pyr-Ru-H 1~4**.

***trans*-Pyr-Ru-H 1**			
Ru(1)-C(11)	1.837(3)	Ru(1)-N(2)	2.138(2)
Ru(1)-N(1)	2.1894(19)	Ru(1)-P(1)	2.3422(7)
Ru(1)-P(2)	2.3435(7)	Ru(1)-H(100)	1.63(2)
O(2)-C(11)	1.161(3)		
C(11)-Ru(1)-N(2)	177.96(8)	N(2)-Ru(1)-N(1)	76.11(8)
P(1)-Ru(1)-P(2)	173.31(2)	N(1)-Ru(1)-H(100)	164.7(9)
***trans*-Pyr-Ru-H 2**			
Ru(1)-C(48)	1.837(2)	Ru(1)-N(2)	2.1521(19)
Ru(1)-N(1)	2.1591(19)	Ru(1)-P(1)	2.3417(6)
Ru(1)-P(2)	2.3545(6)	Ru(1)-H(100)	1.53(2)
O(1)-C(48)	1.162(3)		
C(48)-Ru(1)-N(2)	175.92(9)	N(2)-Ru(1)-N(1)	76.45(7)
P(1)-Ru(1)-P(2)	176.33(2)	N(1)-Ru(1)-H(100)	164.4(10)
***cis*-Pyr-Ru-H 2**			
Ru(1)-C(60)	1.837(5)	Ru(1)-N(1)	2.123(3)
Ru(1)-N(2)	2.169(3)	Ru(1)-P(2)	2.3362(11)
Ru(1)-P(1)	2.3624(11)	O(1)-C(60)	1.159(4)
Ru(1)-H(101)	1.6040		
C(60)-Ru(1)-N(1)	173.32(16)	N(1)-Ru(1)-N(2)	76.96(12)
P(2)-Ru(1)-P(1)	168.70(4)	N(2)-Ru(1)-H(101)	166.7
***cis*-Pyr-Ru-H 3**			
Ru(1)-C(12)	1.845(2)	Ru(1)-N(1)	2.1178(19)
Ru(1)-N(2)	2.185(2)	Ru(1)-P(2)	2.3438(6)
Ru(1)-P(1)	2.3575(6)	Ru(1)-H(41)	1.57(3)
O(1)-C(12)	1.154(3)		
C(12)-Ru(1)-N(1)	176.79(9)	N(1)-Ru(1)-N(2)	76.18(8)
P(2)-Ru(1)-P(1)	169.15(2)	N(2)-Ru(1)-H(41)	169.2(10)
***cis*-Pyr-Ru-H 4**			
Ru(1)-C(10)	1.826(5)	Ru(1)-N(1)	2.155(4)
Ru(1)-N(2)	2.241(4)	Ru(1)-P(2)	2.3439(16)
Ru(1)-P(1)	2.3577(16)	Ru(1)-H(44)	1.53(4)
O(1)-C(10)	1.170(6)		
C(10)-Ru(1)-N(1)	175.35(19)	N(1)-Ru(1)-N(2)	76.63(14)
P(2)-Ru(1)-P(1)	161.71(5)	N(2)-Ru(1)-H(44)	172.2(15)

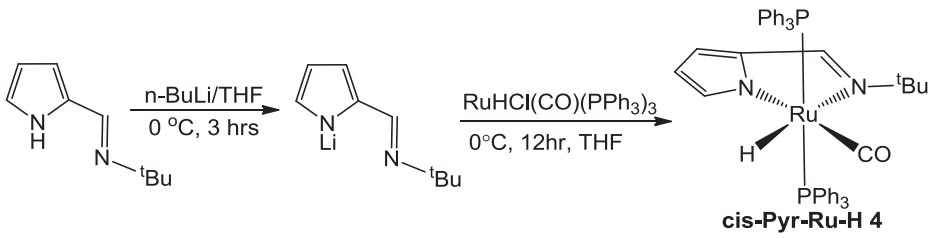

Scheme 3. Synthesis of complex ***cis*-Pyr-Ru-H 4**.

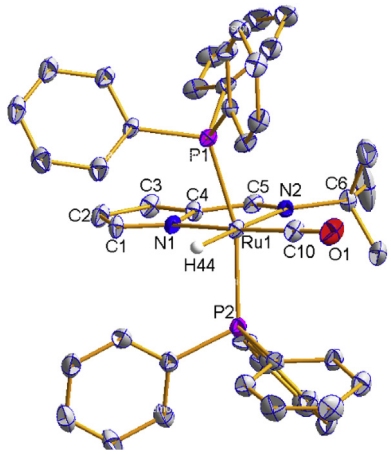

Fig. 8. Molecular geometry of ***cis*-Pyr-Ru-H 4**. The hydrogen atoms except the hydride were omitted for clarity. Thermal ellipsoids were drawn at 30% probabilities.

the geometries of ruthenium complexes and their relative stabilities. The question of which geometry is the real active form for catalytic reactions remains to be answered.

2.5. Catalytic alcohol amination

Secondary and tertiary amines, obtained from the reactions of imine condensation and reductive hydrogenation or from the reaction of amines with alkyl halides, are important in organic synthesis and the pharmaceutical industry [22]. Finding a "green method" for generating substituted amines with higher atom economy and lower energy consumption is a general trend in the current chemistry community. Using organometallic catalysts to catalyze the reaction of alcohol aminations forming substituted amines is under investigation by many research groups and among these studies, ruthenium-based catalysts are quite important [23]. It is believed that the mechanism of alcohol amination is achieved through (a) dehydrogenation of alcohol by ruthenium compounds, (b) imine condensation with amine substrates, and (c) hydrogenation via the

borrowing hydrogen methodology (Scheme 4).

We first tried to understand the relationship between geometries and the catalytic activity. Therefore, we chose to use the thermally stable ***cis*-Pyr-Ru-H 4** as the catalyst for the reaction of benzyl alcohol with aniline. The possible products, *N*-benzylideneaniline and *N*-benzylaniline, were detected and conversion rates were calculated by using ^{1}H NMR spectra. The results showed that ***cis*-Pyr-Ru-H 4** cannot catalyze the amination of benzyl alcohol with aniline even after exposure at 110 °C overnight (as shown in Table 5, Entry 9). When the pure ***cis*-** and ***trans*-Pyr-Ru-H 1**–**3** were used as catalysts, the results in Table 5 showed all the conversions are at ca. 97% after 24 h, according to the ^{1}H NMR spectra. These results imply that pre-heating the ***cis*-** and ***trans*-Pyr-Ru-H 1**–**3** compounds induced geometry isomerization of these compounds and they reached an equilibrium before the benzyl alcohol and aniline were added. The *trans* form of the catalysts are the active catalysts. Reaction time affected the final products of the alcohol amination (Entries 5 and 6). Benzyl alcohol was first dehydrogenated by the catalysts forming benzaldehyde which then reacted with aniline to from *N*-benzylideneaniline via imine condensation. The *N*-benzylideneaniline then was hydrogenated to yield *N*-benzylaniline in the presence of the metal hydride catalysts as shown in Scheme 4(c).

3. Conclusions

Steric hindrance of substituents on the imine group of bidentate pyrrole-imine ligands affected the geometries of ruthenium compounds which also contained hydride and carbonyl groups. When the bulky *t*-butyl group was used as the imine substituent, only ***cis*-Pyr-Ru-H 4** was isolated and no ***trans*-Pyr-Ru-H 4** was observed. In contrast, with smaller imine substituents such as -CH_2-2′-furanyl, -CH_2CH_2-morpholine, and -CH_2-2′-pyridinyl, ***trans*** and ***cis* -Pyr-Ru-H 1**–**3** were observed and isolated. These ***trans*** and ***cis* -Pyr-Ru-H forms** could be interconverted to each other thermodynamically and reached an equilibrium. Catalytic alcohol aminations using these ruthenium compounds showed that only the *trans* form of the ruthenium hydride compounds could catalyze these reactions actively. Presumably, the geometries of ruthenium catalysts blocked the entrances of alcohol to the ruthenium center to form ruthenium alkoxide and the successive steps. These results indicate the importance of geometry of the catalyst.

4. Experimental section

4.1. Materials and physical techniques

The ^{1}H and ^{13}C NMR spectra were recorded using a Bruker Avance 300 spectrometer and the chemical shifts were recorded in ppm relative to the residual protons of $CDCl_3$ ($\delta = 7.24$, 77.0 ppm). External standard of 85% H_3PO_4 was used for ^{31}P NMR chemical shift. Elemental analyses were performed using a Heraeus CHN-OS Rapid Elemental Analyzer at the Instrument Center of the NCHU. Ligands C_4H_3NH(2-CH=NCH_2-2′-furanyl) (**L_1H**) C_4H_3NH(2-CH=NCH_2CH_2-morpholine) (**L_2H**), C_4H_3NH(2-CH=NCH_2-2′-pyridinyl) (**L_3H**) [13], and [RuHCl(CO)(PPh_3)$_3$] [9] are synthesized by modifying the published procedures.

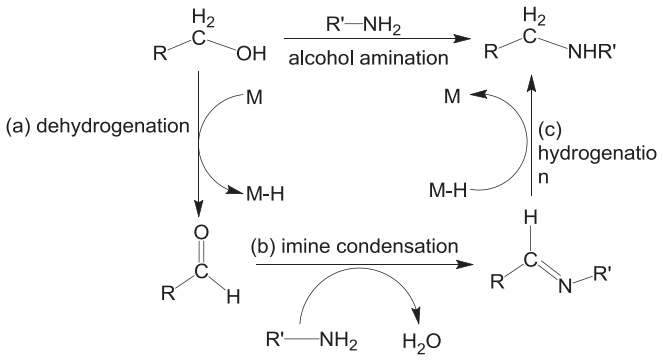

Scheme 4. The plausible mechanism for alcohol amination.

4.2. Synthesis of compounds

4.2.1. Synthesis of trans-Pyr-Ru-H 1

A Schlenk flask containing **L_1H** (0.40 g, 2.3 mmol) and THF (50 mL) was added 2.5 M of n-BuLi (1.01 mL, 2.53 mmol) at −78 °C. The solution was stirred for 4 h at room temperature and added dropwise at 0 °C to another flask which contains RuHCl(CO)(PPh_3)$_3$ (2.18 g, 2.3 mmol) and THF (30 mL). The mixture was stirred at room temperature for 12 h and volatiles were removed under vacuum. The residue was extracted with methylene chloride and filtered through celite. The filtrate was dried again under vacuum and the solid was washed with heptane to remove excess of triphenylphosphine. The remaining solid was recrystallized from a methylene chloride solution at −20 °C to give 0.59 g of final product (31% yield). ^{1}H NMR ($CDCl_3$): 7.27–7.49 (m, 30H, P*Ph*$_3$), 7.12 (s, 1H, C*H* furan), 6.95 (s, 1H, C*H* pyrrole), 6.48 (s, 1H, C*H* imine), 6.23 (m, 1H, C*H* pyrrole), 6.08 (s, 1H, C*H* furan), 5.92 (m, 1H, C*H* pyrrole), 5.32 (m, 1H, C*H* furan), 3.64 (s, 2H, CH_2), −11.34 (t, $^2J_{HP} = 19.5$ Hz, 1H, Ru*H*). ^{13}C{^{1}H} NMR ($CDCl_3$): 206.2 (t, $J_{CP} = 16.0$ Hz, *C*O), 157.1 (*C*H imine), 150.9 (*C* furan), 142.1 (*C*H furan), 140.5 (*C* pyrrole), 139.5 (*C*H pyrrole), 134.5 (t, $J_{CP} = 5.9$ Hz, *C*H PPh$_3$), 134.1 (vt, $J_{CP} = 20.4$ Hz, *C* PPh$_3$), 129.5 (*C*H PPh$_3$), 127.9 (t, $J_{CP} = 4.5$ Hz, *C*H PPh$_3$), 115.1 (*C*H pyrrole), 111.1 (*C*H pyrrole), 110.6 (*C*H furan), 110.1 (*C*H furan), 55.5 (*C*H$_2$). ^{31}P NMR ($CDCl_3$): 46.5 (d, $^2J_{HP} = 19.5$ Hz, PPh$_3$). IR (KBr, cm^{-1}): $\nu = 1901$ (CO). Anal. Calcd. for $RuC_{47}H_{40}N_2O_2P_2$: Calcd.: C: 68.19, H: 4.87, N: 3.38. Found: C: 68.04, H: 4.94, N: 3.54.

4.2.2. Synthesis of cis-Pyr-Ru-H 1

Same procedures used as for synthesizing ***trans*-Pyr-Ru-H 1** are adopted except the solution of RuHCl(CO)(PPh_3)$_3$ and the lithium reagent of **L_1H** was refluxed for 24 h. Successively purification procedures are same as that for purifying compound **1**. White crystals of ***cis*-Pyr-Ru-H 1** was obtained from a saturated methylene chloride/heptane solution at −20 °C (0.86 g, 45%). ^{1}H NMR ($CDCl_3$): 7.22–7.31 (m, 30H, P*Ph*$_3$), 7.14 (s, 1H, C*H* furan), 6.89 (s, 1H, C*H* imine), 6.29 (s, 1H, C*H* pyrrole), 6.18 (m, 1H, C*H* furan), 5.94 (s, 1H, C*H* pyrrole), 5.69 (mz, 1H, C*H* pyrrole), 5.68 (m, 1H, C*H* furan), 4.11 (s, 2H, CH_2), −10.74 (t, $^2J_{HP} = 21.6$ Hz, 1H, Ru*H*). ^{13}C{^{1}H} NMR ($CDCl_3$): 206.1 (t, $J_{CP} = 14.0$ Hz, *C*O), 155.8 (*C*H imine), 151.8 (*C* furan), 142.3 (*C*H furan), 141.2 (*C* pyrrole), 138.6 (*C*H pyrrole), 134.4 (vt, $J_{CP} = 20.5$ Hz, *C*H PPh$_3$), 134.0 (t, $J_{CP} = 6.0$ Hz, *C* PPh$_3$), 129.2 (*C*H PPh$_3$), 127.9 (t, $J_{CP} = 4.4$ Hz, *C*H PPh$_3$), 114.5 (*C*H pyrrole), 111.5 (*C*H pyrrole), 110.2 (*C*H furan), 109.7 (*C*H furan), 55.8 (*C*H$_2$). ^{31}P NMR ($CDCl_3$): 47.5 (d, $^2J_{HP} = 21.6$ Hz, PPh$_3$). IR (KBr, cm^{-1}): $\nu = 1916$ (CO). Anal. Calcd. for $RuC_{47}H_{40}N_2O_2P_2$: Calcd.: C: 68.19, H: 4.87, N: 3.38. Found: C: 68.09, H: 4.39, N: 3.42.

4.2.3. Synthesis of trans-Pyr-Ru-H 2

Similar procedures used as for synthesizing ***trans*-Pyr-Ru-H 1** are adopted. Reactants **L_2H** (0.40 g, 1.93 mmol), 2.5 M of n-BuLi (0.85 mL, 2.12 mmol), RuHCl(CO)(PPh_3)$_3$ (1.84 g, 1.93 mmol) were used. Compound ***trans*-Pyr-Ru-H 2** was recrystallized from dichloromethane/DMSO solution in 39% yield (0.654 g). ^{1}H NMR ($CDCl_3$): 7.24–7.45 (m, 30H, P*Ph*$_3$), 6.96 (s, 1H, C*H* imine), 6.77 (s, 1H, C*H* pyrrole), 6.43 (m, 1H, C*H* pyrrole), 5.94 (m, 1H, C*H* pyrrole),

Table 5
Catalytic amination of benzyl alcohol with aniline[a].

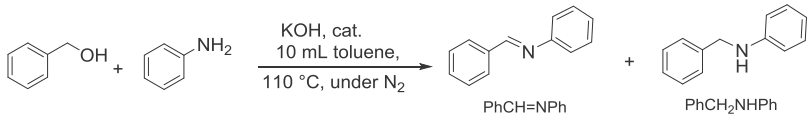

Entry	Cat.	mol%	Time (h)	Conv. (%)	PhCH = NPh: $PhCH_2NHPh$
1	–		12	trace	
2	***trans*-Pyr-Ru-H 1**	0.5	24	97	3:97
3	***cis*-Pyr-Ru-H 1**	0.5	24	97	12:88
4	***trans*-Pyr-Ru-H 2**	0.5	24	97	10:90
5	***cis*-Pyr-Ru-H 2**	0.5	12	97	32:68
6	***cis*-Pyr-Ru-H 2**	0.5	24	97	20:80
7	***trans*-Pyr-Ru-H 3**	0.5	24	97	8:92
8	***cis*-Pyr-Ru-H 3**	0.5	24	97	6:94
9	***cis*-Pyr-Ru-H 4**	0.5	24	0	0

[a] Reaction condition: aniline (4 mmol)/benzyl alcohol (4 mmol)/catalyst/KOH (8 mmol) in toluene at 110 °C.

3.50–3.53 (m, 4H, C*H*$_2$O morpholine), 2.51–2.57 (m, 2H, C*H*$_2$), 1.91–1.94 (m, 4H, C*H*$_2$N morpholine), 1.39–1.45 (m, 2H, C*H*$_2$), −11.43 (t, $^2J_{HP}$ = 18.9 Hz, 1H, Ru*H*). $^{13}C\{^1H\}$ NMR ($CDCl_3$): 206.0 (t, J_{CP} = 16.5 Hz, *C*O), 158.7 (*C*H imine), 140.3 (*C* pyrrole), 139.6 (*C*H pyrrole), 134.5 (t, J_{CP} = 5.8 Hz, *C*H PPh_3), 134.0 (vt, J_{CP} = 20.6 Hz, *C* PPh_3), 129.5 (*C*H PPh_3), 127.8 (t, J_{CP} = 4.5 Hz, *C*H PPh_3), 114.8 (*C*H pyrrole), 111.2 (*C*H pyrrole), 66.9 (CH_2 morpholine), 57.7 (*C*H$_2$), 57.4 (*C*H$_2$), 53.8 (CH_2 morpholine). ^{31}P NMR ($CDCl_3$): 46.8 (d, $^2J_{HP}$ = 18.9 Hz, PPh_3). IR (KBr, cm^{-1}): ν = 1905 (CO). Small amount of methylene chloride was packed in crystals resulting inaccurate for the elemental analysis.

4.2.4. Synthesis of cis-Pyr-Ru-H 2

Similar procedures used as for synthesizing ***cis*-Pyr-Ru-H 1** are adopted. Reactants **L_2H** (0.40 g, 1.93 mmol), 2.5 M of n-BuLi (0.85 mL, 2.12 mmol), $RuHCl(CO)(PPh_3)_3$ (1.84 g, 1.93 mmol) were used. Compound ***cis*-Pyr-Ru-H 2** was recrystallized from dichloromethane/DMSO solution in 42% yield (0.70 g). ^1H NMR ($CDCl_3$): 7.19–7.34 (m, 30H, P*Ph*$_3$), 7.18 (s, 1H, C*H* imine), 6.35 (s, 1H, C*H* pyrrole), 5.82 (m, 1H, C*H* pyrrole), 5.66 (m, 1H, C*H* pyrrole), 3.59–3.62 (m, 4H, C*H*$_2$O morpholine), 3.07–3.12 (m, 2H, C*H*$_2$), 2.16 (m, 4H, C*H*$_2$N morpholine), 1.74–1.79 (m, 2H, C*H*$_2$), −10.80 (t, $^2J_{HP}$ = 21.9 Hz, 1H, Ru*H*). $^{13}C\{^1H\}$ NMR ($CDCl_3$): 206.5 (t, J_{CP} = 13.8 Hz, *C*O), 157.1 (*C*H imine), 141.3 (*C* pyrrole), 138.6 (*C*H pyrrole), 134.3 (vt, J_{CP} = 20.6 Hz, *C* PPh_3), 134.0 (t, J_{CP} = 5.9 Hz, *C*H PPh_3), 129.2 (*C*H PPh_3), 127.8 (t, J_{CP} = 4.5 Hz, *C*H PPh_3), 113.9 (*C*H pyrrole), 111.1 (*C*H pyrrole), 67.0 (CH_2 morpholine), 59.0 (*C*H$_2$), 57.8 (*C*H$_2$), 53.9 (CH_2 morpholine). ^{31}P NMR ($CDCl_3$): 47.5 (d, $^2J_{HP}$ = 21.9 Hz, PPh_3). IR (KBr, cm^{-1}): ν = 1913 (CO). Anal. Calcd. for $RuC_{49}H_{47}N_3O_2P_2$: Calcd.: C: 66.89, H: 5.61, N: 4.88. Found: C: 65.72, H: 5.26, N: 4.80. Small amount of solvent was packed in crystals resulting inaccurate for the elemental analysis.

4.2.5. Synthesis of trans-Pyr-Ru-H 3

Similar procedures used as for synthesizing ***trans*-Pyr-Ru-H 1** are adopted. Reactants **L_3H** (0.40 g, 2.16 mmol), 2.5 M of n-BuLi (0.95 mL, 2.38 mmol), $RuHCl(CO)(PPh_3)_3$ (2.06 g, 2.16 mmol) were used. Compound ***trans*-Pyr-Ru-H 3** was obtained in 36% yield (0.64 g). ^1H NMR ($CDCl_3$): 8.33 (s, 1H, C*H* pyridine), 7.22–8.31 (m, 30H, P*Ph*$_3$), 6.89–7.08 (m, 3H, C*H* pyridine+pyrrole), 6.87 (s, 1H, C*H* imine), 6.31 (m, 1H, C*H* pyridine), 6.22 (s, 1H, C*H* pyrrole), 5.95 (m, 1H, C*H* pyrrole), 3.88 (s, 2H, C*H*$_2$), −11.31 (t, $^2J_{HP}$ = 18.9 Hz, 1H, Ru*H*). $^{13}C\{^1H\}$ NMR ($CDCl_3$): 206.2 (t, J_{CP} = 16.8 Hz, *C*O), 159.6 (*C*H imine), 156.9 (*C* pyridine), 149.1 (*C*H pyridine), 140.7 (*C* pyrrole), 139.3 (*C*H pyrrole), 135.6 (*C*H pyridine), 134.5 (t, J_{CP} = 6.1 Hz, *C*H PPh_3), 134.1 (vt, J_{CP} = 20.6 Hz, *C* PPh_3), 129.4 (*C*H PPh_3), 127.8 (t, J_{CP} = 4.5 Hz, *C*H PPh_3), 124.8 (*C*H pyridine), 122.1 (*C*H pyridine), 115.4 (*C*H pyrrole), 111.3 (*C*H pyrrole), 66.8 (*C*H$_2$). ^{31}P NMR ($CDCl_3$): 45.5 (d, $^2J_{HP}$ = 18.9 Hz, PPh_3). IR (KBr, cm^{-1}): ν = 1901 (CO). Anal. Calcd. for $RuC_{48}H_{41}N_3OP_2$: Calcd.: C: 68.72, H: 4.93, N: 5.01. Found: C: 66.92, H: 4.67, N: 4.94. Small amount of solvent was packed in crystals resulting inaccurate for the elemental analysis.

4.2.6. Synthesis of cis-Pyr-Ru-H 3

Similar procedures used as for synthesizing ***cis*-Pyr-Ru-H 1** are adopted. Reactants **L_3H** (0.40 g, 2.16 mmol), 2.5 M of n-BuLi (0.95 mL, 2.38 mmol), $RuHCl(CO)(PPh_3)_3$ (2.06 g, 2.16 mmol) were used. Compound ***cis*-Pyr-Ru-H 3** was obtained in 46% yield (0.83 g). ^1H NMR ($CDCl_3$): 8.41 (m, 1H, C*H* pyridine), 7.25 (s, CH imine), 7.16–7.30 (m, 31H, pyridine+P*Ph*$_3$), 7.00 (m, 1H, C*H* pyridine), 6.40 (m, 1H, C*H* pyrrole), 6.31 (m, 1H, C*H* pyridine), 5.90 (m, 1H, C*H* pyrrole), 5.72 (m, 1H, C*H* pyrrole), 4.39 (s, 2H, C*H*$_2$), −10.93 (t, $^2J_{HP}$ = 22.2 Hz, 1H, Ru*H*). $^{13}C\{^1H\}$ NMR ($CDCl_3$): 205.9 (t, J_{CP} = 13.7 Hz, *C*O), 158.6 (*C* pyridine), 158.2 (*C*H imine), 149.2 (*C*H pyridine), 141.4 (*C* pyrrole), 138.6 (*C*H pyrrole), 136.4 (*C*H pyridine), 134.4 (vt, J_{CP} = 20.6 Hz, *C* PPh_3), 134.0 (t, J_{CP} = 5.8 Hz, *C*H PPh_3), 129.2 (*C*H PPh_3), 127.8 (t, J_{CP} = 4.5 Hz, *C*H PPh_3), 123.2 (*C*H pyridine), 121.8 (*C*H pyridine), 114.8 (*C*H pyrrole), 111.6 (*C*H pyrrole), 67.3 (*C*H$_2$). ^{31}P NMR ($CDCl_3$): 46.5 (d, $^2J_{HP}$ = 22.2 Hz, PPh_3). IR (KBr, cm^{-1}): ν = 1914 (CO), 1940 (Ru-H). Small amount of solvent was packed in crystals resulting inaccurate for the elemental analysis.

4.2.7. Synthesis of cis-Pyr-Ru-H 4

Similar procedures used as for synthesizing ***cis*-Pyr-Ru-H 1** are adopted. Reactants **L_4H** (0.10 g, 0.67 mmol), 2.5 M of n-BuLi (0.32 mL, 0.80 mmol), $RuHCl(CO)(PPh_3)_3$ (0.64 g, 0.57 mmol) were used. Compound ***cis*-Pyr-Ru-H 4** was obtained in 74% yield (0.34 g). ^1H NMR ($CDCl_3$): 7.52 (s, CH imine), 7.20–7.33 (m, 30H, P*Ph*$_3$), 6.47 (m, 1H, C*H* pyrrole), 5.63 (m, 1H, C*H* pyrrole), 5.60 (m, 1H, C*H* pyrrole), 0.89 (s, 9H, ^{t}*Bu*), −12.08 (t, $^2J_{HP}$ = 24 Hz, 1H, Ru*H*). $^{13}C\{^1H\}$ NMR ($CDCl_3$): 153.7 (*C*H imine), 142.4 (*C* pyrrole), 138.0 (*C*H pyrrole), 134.4 (vt, J_{CP} = 20.6 Hz, *C* PPh_3), 134.0 (t, J_{CP} = 6 Hz, *C*H PPh_3), 129.3 (*C*H PPh_3), 127.8 (t, J_{CP} = 4.5 Hz, *C*H PPh_3), 114.1 (*C*H pyrrole), 110.6 (*C*H pyrrole), 59.2 (*C* ^{t}Bu), 31.5 (*Me* ^{t}Bu). ^{31}P NMR ($CDCl_3$): 44.5 (d, $^2J_{HP}$ = 24 Hz, PPh_3). IR (KBr, cm^{-1}): ν = 1924 (CO), 2109 (Ru-H). Small amount of solvent was packed in crystals resulting inaccurate for the elemental analysis.

4.3. General procedure for catalytic alcohol amination

Under nitrogen atmosphere, a mixture of KOH (8.0 mmol) and catalyst in toluene (10 mL) was heated at 110 °C for 2hr in order to reach equilibrium for the *cis* and *trans* forms of the complexes. A toluene solution (10 ml) of benzyl alcohol (4.0 mmol) and aniline (4.0 mmol) was added. The mixture was heated at 110 °C for a period of time. Small amount of samples (ca. 0.5 mL) were drawn from the reaction flask via syringe during the reactions. The products were analyzed by ^{1}HNMR spectra using the integrations of methylene protons of N-benzylideneaniline, N-benzylaniline, and N-benzylaniline (δ 8.45, 4.32, 4.60) for calculating the conversions.

4.4. X-ray structure determination

All of the crystals were mounted on a glass fiber using epoxy resin and *trans*ferred to a goniostat. The data were collected on a Bruker SMART CCD diffractometer using graphite monochromated Mo-K_α radiation. The data were corrected for absorption empirically via ψ scans. All non-hydrogen atoms were refined using anisotropic displacement parameters. For all of the structures, the hydrogen atom positions were calculated, and they were constrained to idealized geometries and treated as riding where the H atom displacement parameter was calculated from the equivalent isotropic displacement parameter of the bound atom. The structures were determined using direct-method procedures in SHELXS [24] and refined using full-matrix least-squares methods on F^2's in SHELXL [25]. All the relevant crystallographic data and structure refinement parameters are summarized in Table 1. The crystallographic data for the structures reported in this paper have been deposited with the Cambridge Crystallographic Data Centre as supplementary publications nos. CCDC-1845663 (***trans*-Pyr-Ru-H 1**), CCDC- 1873675 (***trans*-Pyr-Ru-H 2**), CCDC-1873939 (***cis*-Pyr-Ru-H 1**), CCDC-1873940 (***cis*-Pyr-Ru-H 2**), CCDC-1873941 (***cis*-Pyr-Ru-H 3**), and CCDC-1873942 (***cis*-Pyr-Ru-H 4**). These data can be obtained free of charge from The Cambridge Crystallographic Data Centre via www.ccdc.cam.ac.uk/data_request/cif.

Acknowledgements

This work is supported by the Ministry of Science and Technology of Taiwan. We also thank the National Changhua University of Education for supporting the X-ray diffractometer and NMR spectrometer. The financial support of the Conquest software and Web CSD from National Center for High-performance Computing of Taiwan is also acknowledged.

Appendix A. Supplementary data

Supplementary data related to this article can be found at https://doi.org/10.1016/j.jorganchem.2019.120957.

References

[1] (a) S.Y. de Boer, T.J. Korstanje, S.R. La Rooij, R. Kox, J.N.H. Reek, J.I. van der Vlugt, Organometallics 36 (2017) 1541–1549;
(b) K.-N.T. Tseng, J.W. Kampf, N.K. Szymczak, ACS Catal. 5 (2015) 5468–5485;
(c) C. Gunanathan, D. Milstein, Chem. Rev. 114 (2014) 12024–12087;
(d) B. Pan, B. Liu, E. Yue, Q. Liu, X. Yang, Z. Wang, W.-H. Sun, ACS Catal. 6 (2016) 1247–1253.

[2] (a) Y. Ogiwara, M. Miyake, T. Kochi, F. Kakiuchi, Organometallics 36 (2017) 159–164;
(b) M.K. Awasthi, D. Tyagi, S. Patra, R.K. Rai, S.M. Mobin, S.K. Singh, Chem. Asian J. 13 (2018) 1424–1431;
(c) O. Ogata, H. Nara, M. Fujiwhara, K. Matsumura, Y. Kayaki, Org. Lett. 20 (2018) 3866–3870.

[3] (a) M. Ramesh, G. Prabusankar, G. Venkatachalam, Inorg. Chem. Commun. 79 (2017) 89–94;
(b) S. Ramakrishnan, K.M. Waldie, I. Warnke, A.G. De Crisci, V.S. Batista, R.M. Waymouth, C.E.D. Chidsey, Inorg. Chem. 55 (2016) 1623–1632;
(c) K. Abdur-Rashid, R. Abbel, A. Hadzovic, A.J. Lough, R.H. Morris, Inorg. Chem. 44 (2005) 2483–2492;
(d) W. Xu, R. Langer, Dalton Trans. 44 (2015) 16785–16790.

[4] (a) N. Nakagawa, E.J. Derrah, M. Schelwies, F. Rominger, O. Trapp, T. Schaub, Dalton Trans. 45 (2016) 6856–6865;
(b) D. Pingen, M. Lutz, D. Vogt, Organometallics 33 (2014) 1623–1629;
(c) D. Pingen, J.H. Choi, H. Allen, G. Murray, P. Ganji, P.W.N.M. Van Leeuwen, M.H.G. Prechtl, D. Vogt, Catal. Sci. Technol. 8 (2018) 3969–3976;
(d) G. Choi, S.H. Hing, Angew. Chem. Int. Ed. 57 (2018) 6166–6170;
(e) T. Yan, B.L. Feringa, K. Barta, Sci. Adv. 3 (2017), eaao6494.

[5] (a) R. da Silva Vidal, F.G. Doro, K.Q. Ferreira, Z.N. da Rocha, E.E. Castellano, S. Nikolaou, E. Tfouni, Inorg. Chem. Commun. 15 (2012) 93–96;
(b) A. Gavriluta, G.E. Büchel, L. Freitag, G. Novitchi, J.B. Tommasino, E. Jeanneau, P.-S. Kuhn, L. González, V.B. Arion, D. Luneau, Inorg. Chem. 52 (2013) 6260–6272;
(c) D. Schott, C.J. Sleigh, J.P. Lowe, S.B. Duckett, R.J. Mawby, M. Partridge, Inorg. Chem. 41 (2002) 2960–2970.

[6] (a) A. Merlino, Coord. Chem. Rev. 326 (2016) 111–134;
(b) P. Kumar, R.K. Gupta, D.S. Pandey, Chem. Soc. Rev. 43 (2014) 707–733;
(c) A. Koceva-Chyła, K. Matczak, P. Hikisz, K. Durka, K. Kochel, G. Süss-Fink, J. Furrer, K. Kowalski, ChemMedChem 11 (2016) 2171–2187;
(d) S. Thota, D.A. Rodrigues, D.C. Crans, E.J. Barreiro, J. Med. Chem. 61 (2018) 5805–5821.

[7] (a) J.-P. Djukic, J.-B. Sortais, L. Barloy, M. Pfeffer, Eur. J. Inorg. Chem. (2009) 817–853;
(b) C. Gunanathan, D. Milstein, Chem. Rev. 114 (2014) 12024–12087;
(c) C.P. Lau, S.M. Ng, G. Jia, Z. Lin, Coord. Chem. Rev. 251 (2007) 2223–2227;
(d) E. Khaskin, M.A. Iron, L.J.W. Shimon, J. Zhang, D. Milstein, J. Am. Chem. Soc. 132 (2010) 8542–8543.

[8] (a) W. Grochala, P.P. Edwards, Chem. Rev. 104 (2004) 1283–1315;
(b) S. Nag, R.J. Butcher, S. Bhattacharya, Eur. J. Inorg. Chem. (2007) 1251–1260.

[9] N. Ahmad, J.J. Levison, S.D. Robinson, M.F. Uttley, Inorg. Synth. 15 (1974) 45–64.

[10] (a) A.G. Nair, R.T. McBurney, D.B. Walker, M.J. Page, M.R.D. Gatus, M. Bhadbhade, B.A. Messerle, Dalton Trans. 45 (2016) 14335–14342;
(b) F. Yu, W.-K. Chu, C. Shen, Y. Luo, J. Xiang, S.-Q. Chen, C.-C. Ko, T.-C. Lau, Eur. J. Inorg. Chem. (2016) 3892–3899;
(c) M. Trivedi, M. Chandra, D.S. Pandey, M.C. Puerta, P. Valerga, J. Organomet. Chem. 689 (2004) 879–882.

[11] (a) R.F.R. Jazzar, S.A. Macgregor, M.F. Mahon, S.P. Richards, M.K. Whittlesey, J. Am. Chem. Soc. 124 (2002) 4944–4945;
(b) T.N. Choo, W.-H. Kwok, C.E.F. Rickard, W.R. Roper, L.J. Wright, J. Organomet. Chem. 645 (2002) 235–245;
(c) S. Burling, B.M. Paine, D. Nama, V.S. Brown, M.F. Mahon, T.J. Prior, P.S. Pregosin, M.K. Whittlesey, J.M.J. Williams, J. Am. Chem. Soc. 129 (2007) 1987–1995.

[12] (a) L. Casarrubios, M.A. Esteruelas, C. Larramona, J.G. Muntaner, M. Oliván, E. Oñate, M.A. Sierra, Organometallics 33 (2014) 1820;
(b) A. Sarbajna, I. Dutta, P. Daw, S. Dinda, S.M.W. Rahaman, A. Sarkar, J.K. Bera, ACS Catal. 7 (2017) 2786–2790;
(c) M. Shivakumar, K. Pramanik, I. Bhattacharyya, A. Chakravorty, Inorg. Chem. 39 (2000) 4332–4338.

[13] G.-H. Chen, W.-J. Leu, J.-H. Guh, C.-H. Lin, J.-H. Huang, J. Organomet. Chem. 868 (2018) 122–130.

[14] (a) J.G. Małecki, S. Krompiec, A. Maroń, M. Penkala, Polyhedron 48 (2012) 24–30;
(b) C.J.E. Davies, J.P. Lowe, M.F. Mahon, R.C. Poulten, M.K. Whittlesey, Organometallics 32 (2013) 4927–4937.

[15] (a) S. Naeem, A.L. Thompson, A.J.P. White, L. Delaudec, J.D.E.T. Wilton-Ely, Dalton Trans. 40 (2011) 3737–3747;
(b) T. Toda, A. Yoshinari, T. Ikariya, S. Kuwata, Chem. Eur J. 22 (2016) 16675–16683;
(c) P. Patel, S. Naeem, A.J.P. White, J.D.E.T. Wilton-Ely, RSC Adv. 2 (2012) 999–1008.

[16] (a) A.W. Verstuyft, J.H. Nelson, L.W. Cary, Inorg. Chem. 15 (1976) 732–734;
(b) R.H. Crabtree, The Organometallic Chemistry of the Transition Metals, fourth ed., John Wiley & Sons, Inc., Hoboken, New Jersey, 2005.

[17] (a) J.B. Letts, T.J. Mazanec, D.W. Meek, J. Am. Chem. Soc. 104 (1982) 3898–3905;
(b) A. Poater, F. Ragone, A. Correa, A. Szadkowska, M. Barbasiewicz, K. Grela, L. Cavallo, Chem. Eur J. 16 (2010) 14354–14364;
(c) H. Amouri, J.B. Waern, R. Caspar, A. Barbieri, C. Sabatini, A. Zanellib, F. Barigelletti, Dalton Trans. (2007) 2179–2186.

[18] Y. Zhao, D.G. Truhlar, J. Phys. Chem. A 110 (2006) 5121–5129.

[19] M.J. Frisch, J.A. Pople, J.S. Binkley, J. Chem. Phys. 80 (1984) 3265–3269.

[20] M.J. Frisch, G.W. Trucks, H.B. Schlegel, G.E. Scuseria, M.A. Robb, J.R. Cheeseman, G. Scalmani, V. Barone, B. Mennucci, G.A. Petersson, H. Nakatsuji, M. Caricato, X. Li, H.P. Hratchian, A.F. Izmaylov, J. Bloino, G. Zheng, J.L. Sonnenberg, M. Hada, M. Ehara, K. Toyota, R. Fukuda, J. Hasegawa, M. Ishida, T. Nakajima, Y. Honda, O. Kitao, H. Nakai, T. Vreven, J.A. Montgomery Jr., J.E. Peralta, F. Ogliaro, M.J. Bearpark, J. Heyd, E.N. Brothers, K.N. Kudin, V.N. Staroverov, R. Kobayashi, J. Normand, K. Raghavachari, A.P. Rendell, J.C. Burant, S.S. Iyengar, J. Tomasi, M. Cossi, N. Rega, N.J. Millam,

M. Klene, J.E. Knox, J.B. Cross, V. Bakken, C. Adamo, J. Jaramillo, R. Gomperts, R.E. Stratmann, O. Yazyev, A.J. Austin, R. Cammi, C. Pomelli, J.W. Ochterski, R.L. Martin, K. Morokuma, V.G. Zakrzewski, G.A. Voth, P. Salvador, J.J. Dannenberg, S. Dapprich, A.D. Daniels, Ö. Farkas, J.B. Foresman, J.V. Ortiz, J. Cioslowski, D.J. Fox, Gaussian 09, Gaussian, Inc., Wallingford, CT, USA, 2009.

[21] (a) H. Sasabe, S. Nakanishi, T. Takata, Inorg. Chem. Commun. 6 (2003) 1140–1143;
(b) Y.-H. Chang, W.-J. Leu, A. Datta, H.-C. Hsiao, C.-H. Lin, J.-H. Guh, J.-H. Huang, Dalton Trans. 44 (2015) 16107–16118;
(c) C. Stern, F. Franceschi, E. Solari, C. Floriani, N. Re, R. Scopelliti, J. Organomet. Chem. 593 (2000) 86–95;
(d) S.D. Drouin, H.M. Foucault, G.P.A. Yap, D.E. Fogg, Can. J. Chem. 83 (2005) 748–754.

[22] (a) S. Bähn, S. Imm, L. Neubeert, M. Zhang, H. Neumann, M. Beller, ChemCatChem 3 (2011) 1853–1864;
(b) M.H.S.A. Hamid, J.M.J. Williams, Chem. Commun. (2007) 725–727;
(c) B.L. Conley, M.K. Pennington-Boggio, E. Boz, T.J. Williams, Chem. Rev. 110 (2010) 2294–2312;
(d) J. Luo, M. Wu, F. Xiao, G. Deng, Tetrahedron Lett. 52 (2011) 2706–2709;
(e) T. Yan, B.L. Feringa, K. Barta, Nat. Commun. 5 (2014) 5602;
(f) F.F. Shi, X. Cui, Catalytic Amination for N-Alkyl Amine Synthesis, Academic Press, Elsevier, 2018.

[23] (a) Q. Yang, Q. Wang, Z. Yu, Chem. Soc. Rev. 44 (2015) 2305–2329;
(b) A. Corma, J. Navas, M.J. Sabater, Chem. Rev. 118 (2018) 1410–1459, and references therein.

[24] G.M. Sheldrick, SHELX97- Programs for Crystal Structure Analysis: Structure Determination (SHELXS), University of Göttingen, Germany, 1997.

[25] G.M. Sheldrick, SHELX97- Programs for Crystal Structure Analysis: Refinement (SHELXL), University of Göttingen, Germany, 1997.